

## VERIFICATION OF A DNS CODE OF HIGH ORDER OF ACCURACY USING THE METHOD OF MANUFACTURED SOLUTIONS

**Homero Ghioti da Silva**

Departamento de Engenharia de Materiais, Aeronáutica e Automobilística  
Escola de Engenharia de São Carlos - Universidade de São Paulo, Brasil  
ghioti@sc.usp.br

**Leandro Franco de Souza**

Departamento de Matemática Aplicada e Estatística  
Instituto de Ciências Matemáticas e de Computação - Universidade de São Paulo, Brasil  
lefraso@icmc.usp.br

**Marcello Augusto Faraco de Medeiros**

Departamento de Engenharia de Materiais, Aeronáutica e Automobilística  
Escola de Engenharia de São Carlos - Universidade de São Paulo, Brasil  
marcello@sc.usp.br

**Abstract.** *This paper presents a discussion of the results of a verification test using an unsteady manufactured solution in a numerical code of high order of accuracy. The verification procedure was performed by introducing a forcing term in the Navier-Stokes equation creating a nonrealistic problem that has an analytical solution. An important advantage of the Method of Manufactured Solutions compared with standard verification procedure is that it allows exercising the full governing equations sustaining the original boundary conditions implemented in the code. Moreover, if the code computes the fictitious problem without programming errors then the conversion of the code to compute the real problem is done only deleting the source term in the Navier-Stokes equations. The numerical solution was compared with the manufactured solution and a mesh convergence test to quantify the order of accuracy of the numeric code was made. As explained in this paper, the mesh convergence test must be carried out for small simulation time. Then simulation of the fictitious problem for a long time simulation also was performed. Therefore, it was possible to verify if programming error grew after a long time simulation.*

**keywords:** *Temporal Numerical Simulation, Verification Test, Method of Manufactured Solutions, High Order Compact Finite Differences, Spectral Method.*

### 1. Introduction

Due the strong technological advance of computers, Computational Fluids Dynamics (CFD) has been a field of great importance in Fluids Mechanics, and became a strong ally of experimental and theoretical studies for the interpretation of physical phenomena.

Numerical codes are developed and utilized by researchers and engineers and they should give confidence that the results of the numerical simulation are a good representation of the problem under study. Therefore the concepts at verification and validation should be applied. Verification and validation are different concepts, where one can not be substituted by other. According to Roache, 1997, verification is a study of numerical code that consists in assuring that the equations chosen to a given model are resolved correctly and validation assures that the chosen equations are adequate to study the physical problem. In other words, a verification test should give confidence that programming error from implementation of equations, of boundary conditions and of the discretization scheme does not affect the accuracy of the numerical solution. On the other hand, comparisons between the numerical solution of the physical problem with theoretical and experimental results that has been documented in the literature can be classified as validation test.

The proposal of the present paper is to discuss some results of a purely mathematical verification test using the Method of Manufactured Solutions (MMS). This test was applied in a numerical code of high order of accuracy that intended for simulating an incompressible two-dimensional flow. The basic idea of the MMS is to introduce a source term in the equations creating a nonrealistic problem that has an analytical solution. After, this manufactured solution can be used for comparisons with numerical results (Shih, 1985; Steinberg e Roache, 1985). An advantage of using the MMS compared with standard verification procedure, such as code-to-code comparison and the simulation of benchmark solutions, is that the MMS is capable of exercising fully the code

and makes it possible to evaluate all of the leading error terms in the discretization of the equations (Roache, 1998). Also using other methods it is not easy to find a solution that satisfies the boundary conditions of the problem under study. On the other hand, using the MMS it is quite simple to create an analytical solution that satisfies these boundary conditions. In general the MMS does not represent a flow that is realistic or physically realizable, but, it can give good confidence of the numerical code performance.

Some of the first researchers that proposed the use of the MMS for the purpose of code verification are Shih, 1985, and Steinberg e Roache, 1985. Already in 1986 the MMS was recommended as a good verification test by editors of the ASME Journal of Fluids Engineering (JFE). They published a brief policy statement requiring that, in a paper that presents numerical simulation, at least minimal attention should be paid to the quantification of numerical accuracy (Roache e White, 1986). Later, the policy statement was expanded and also adopted by other research journals (Freitas, 1993; Roache, 1994; ASME, 1994; AIAA, 1994; Gresho e Taylor, 1994).

The MMS can be applied together with a systematic mesh convergent test. Therefore it is possible to verify the order of accuracy of the solution scheme and it help to eliminate programming mistakes in the code (Roache, 1998). Nevertheless it is hard to assure that the numerical code is totally free of programming errors and that the order of accuracy obtained is the one expected. This is particularly important in typical simulations in engineering as, for example, flows over solids walls (boundary layer, Poiseuille flow, Couette flow, etc) where it is often necessary to use different orders of the approximations to the discretization in the wall normal direction. These cases results in a more complex multi order solution scheme, where it is hard to estimate a priori the order of accuracy to compare with the order of accuracy obtained via mesh convergent test.

A verification of the order of accuracy of a version of the present numerical code, which uses compact finite difference scheme in the streamwise direction, can be found in Silva *et al.*, 2005. The verification of accuracy of the code was performed using a steady manufactured solution. One important conclusion was that the order of accuracy can depend on the chosen manufactured solution. In particular, on the values of the high order derivatives of the manufactured solution. For the present work an unsteady manufactured solution was used and two tests were performed. The first test was done assuming a small simulation time. This fact was necessary because a mesh refinement test in the wall normal direction was performed. Then the order of accuracy of the numerical code was obtained. The second test was done assuming a long simulation time. The objective of the second test was to verify if programming errors, when it exists in the present code, increases in time.

The governing equations were written in a vorticity-velocity formulation only for the disturbances. The base flow was given and kept constant throughout the simulation. Since the flow is periodic in the streamwise direction then spectral method in this direction was used. Therefore the flow was divided into Fourier modes. Compact finite difference methods of 5<sup>th</sup> and 6<sup>th</sup> order of accuracy in the wall normal direction was utilized for every Fourier modes except for the primary Fourier mode, where compact finite difference of 4th and 5<sup>th</sup> order in this same direction was utilized. For the temporal integration a 4th order Runge Kutta scheme was implemented. The present numerical code was developed to simulate the linear and nonlinear evolution of unsteady infinitesimal disturbance propagating in a plane Poiseuille flow. Moreover, modulated waves as the wavepackets type will be simulated. Some numerical results obtained via the present code were compared with the Linear Stability Theory (LST) and presented in Crepaldi *et al.*, 2006.

The organization of the paper is as follow. Section 2 presents the formulation and the boundary conditions adopted in the current work. Section 3 gives the verification procedure using the MMS together with a mesh convergent test and the results obtained. Section 4 gives some final remarks.

## 2. Formulation

### 2.1. Governing Equations

In the current work the governing equations for an incompressible two-dimensional flow were written in a vorticity-velocity formulation. The velocity components  $\tilde{u}$  and  $\tilde{v}$  and the spanwise vorticity  $\tilde{\omega}_z$  were written in the following form:

$$\tilde{u} = u_B + u; \quad \tilde{v} = v_B + v; \quad \tilde{\omega}_z = \omega_{zB} + \omega_z, \quad (1)$$

where the terms with subscript  $B$  and the terms without subscripts represent the base flow (Poiseuille) and the disturbance components respectively.

Substituting the expression (1) in the spanwise vorticity transport equation and canceling the terms that satisfy the Poiseuille solution, one obtains the Navier-Stokes equation in a disturbance formulation:

$$\frac{\partial \omega_z}{\partial t} + \frac{\partial a}{\partial x} + \frac{\partial b}{\partial y} = \frac{1}{Re} \left( \frac{\partial^2 \omega_z}{\partial x^2} + \frac{\partial^2 \omega_z}{\partial y^2} \right), \quad (2)$$

where  $a = u_B \omega_z + u \omega_{zB} + u \omega_z$  and  $b = v \omega_{zB} + v \omega_z$  are the nonlinear terms.

The continuity equation is

$$\frac{\partial u}{\partial x} + \frac{\partial v}{\partial y} = 0. \quad (3)$$

Taking the  $y$ -derivative of the continuity equation and of the spanwise vorticity

$$\omega_z = \frac{\partial u}{\partial y} - \frac{\partial v}{\partial x}, \quad (4)$$

one finds a Poisson equation for  $v$ ,

$$\frac{\partial^2 v}{\partial x^2} + \frac{\partial^2 v}{\partial y^2} = -\frac{\partial \omega_z}{\partial x}. \quad (5)$$

An analogous scheme can be used to obtain

$$\frac{\partial^2 u}{\partial y^2} - \frac{\partial^2 v}{\partial x \partial y} = \frac{\partial \omega_z}{\partial y} \quad (6)$$

which was used to calculate the  $u$ . More details of this formulation in a three-dimensional version can be found in Marxen, 1998.

The above equations were made dimensionless using the following reference parameters:  $U_{max}$ , which is the maximum value of velocity in the channel, and  $H$ , which is half the channel height. These variables produce the following dimensionless parameters:

$$x = \frac{x^*}{H}, \quad y = \frac{y^*}{H}, \quad u = \frac{u^*}{U_{max}}, \quad v = \frac{v^*}{U_{max}}, \quad \omega_z = \omega_z^* \frac{H}{U_{max}}, \quad t = t^* \frac{U_{max}}{H},$$

where the terms with an asterisk are dimensional. The Reynolds number (Re) is  $\frac{U_{max}H}{\nu}$ , where  $\nu$  denotes the kinematic viscosity.

## 2.2. Boundary Conditions

A periodic boundary condition was adopted in the streamwise direction ( $x$ -direction) and for the wall normal direction ( $y$ -direction) a non-slip and impermeability ( $u = v = 0$  in the walls) conditions were imposed. The flow geometry is presented in fig. 1.

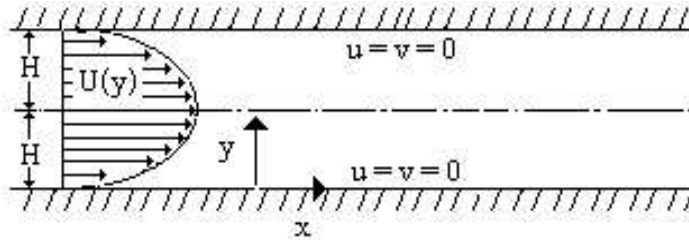


Figure 1: Schematic diagram of physical system

A crucial problem of the vorticity-velocity formulation is that there are no explicit boundary conditions for the vorticity at the wall. It must be computed from the velocity field assuring that the boundary conditions for the velocity are satisfied maintaining consistency and conservation of mass. The calculation of the vorticity at the wall was performed via the equations (5) and (6) and using the fact  $\frac{\partial v}{\partial x} = 0$  at the wall.

### 2.3. Numerical Method

In the  $x$ -direction, a spectral method was used. In this method, a generic quantity  $s$  can be decomposed in Fourier modes ( $\alpha_k$ ) of the following form:

$$s(x, y, t) = \sum_{k=0}^K S_k(y, t) e^{-i\alpha_k x}, \quad (7)$$

where  $s$  represents the variables  $u$ ,  $v$ ,  $w_z$  and  $a$  and  $b$  of equation (2).  $S_k$  represents the discrete Fourier components of the function  $s$ .

Substituting equation (7) in equations (2), (5) and (6) one obtains

$$\frac{\partial \Omega_{z_k}}{\partial t} + i\alpha_k A_k + \frac{\partial B_k}{\partial y} = \frac{1}{Re} (-\alpha_k^2 \Omega_{z_k} + \frac{\partial^2 \Omega_z}{\partial y^2}), \quad (8)$$

$$\frac{\partial^2 V_k}{\partial y^2} - \alpha_k^2 V_k = -i\alpha_k \Omega_{z_k}, \quad (9)$$

$$\frac{\partial^2 U_k}{\partial y^2} = \frac{\partial \Omega_{z_k}}{\partial y} + i\alpha_k \frac{\partial V_k}{\partial y}. \quad (10)$$

All the Fourier modes  $\alpha_k$  (except the primary Fourier mode  $\alpha_0 = 0$ ) were calculated independently using the equations (8) to (10). The primary Fourier mode calculation  $\alpha_0 = 0$  was presented in 2.3.1.

In the  $y$ -direction, a compact finite difference scheme was used. At the points in the interior of the domain, the discretization scheme used centered compact finite difference of 6<sup>th</sup> order of accuracy. For the points in and near wall boundaries, asymmetric schemes of 5<sup>th</sup> and 6<sup>th</sup> order of accuracy were adopted, except to the wall vorticity calculation, where compact finite difference of 6<sup>th</sup> order of accuracy was used. Full Details of the chosen finite differences can be found in Souza *et al.*, 2005. The chosen finite differences for the calculations in the  $y$ -direction when  $\alpha_0 = 0$  was presented in 2.3.1.

#### 2.3.1. The Primary Fourier Mode $\alpha_0$

Making  $\alpha_0 = 0$  in the equations (8) to (10), one obtains the following equations:

$$\frac{\partial \Omega_{z_0}}{\partial t} + \frac{\partial B_0}{\partial y} = \frac{1}{Re} \left( \frac{\partial^2 \Omega_{z_0}}{\partial y^2} \right), \quad (11)$$

$$\frac{\partial^2 V_0}{\partial y^2} = 0, \quad (12)$$

$$\frac{\partial^2 U_0}{\partial y^2} = \frac{\partial \Omega_{z_0}}{\partial y}. \quad (13)$$

The equation (11) was used to calculation  $\Omega_{z_0}$  only at the interior of the domain. The equation (12) together with the impermeability condition resulted in  $V_0 = 0$  for every domain. The equation (13) was used to calculation  $U_0$  for every domain. Since there is no boundary condition for  $\Omega_{z_0}$  at the wall, it was calculated using the vorticity definition equation

$$\Omega_{z_0} = \frac{\partial U_0}{\partial y}. \quad (14)$$

Note that the equation (14) cannot precede the equation (13) and vice-versa. Rather, the equations (13) and (14) should be calculated simultaneously. Two different forms to calculation the equations (13) and (14) were used. The first was an iterative procedure between the equations (13) and (14). But it resulted in a numerical instability. Another form to calculate the equations (13) and (14) was done calculating the equation

(13) independently of the  $\Omega_{z_0}$  calculation at the wall. For this case, the discretization of the term  $\frac{\partial \Omega_{z_0}}{\partial y}$  in the equation (13) was done using the following finite difference:

For the boundary point ( $y = 0$ ) the following noncentered approximation was adopted:

$$-12 \frac{\partial \Omega_{z_0}}{\partial y} \Big|_1 + 137 \frac{\partial \Omega_{z_0}}{\partial y} \Big|_2 = \frac{-25010\Omega_{z_{02}} + 40080\Omega_{z_{03}} - 21240\Omega_{z_{04}} + 7280\Omega_{z_{05}} - 1110\Omega_{z_{06}}}{120\Delta y} + O(\Delta y^4). \quad (15)$$

The near boundary point approximation was:

$$\frac{\partial \Omega_{z_0}}{\partial y} \Big|_2 + 5 \frac{\partial \Omega_{z_0}}{\partial y} \Big|_3 = \frac{-2364\Omega_{z_{02}} - 300\Omega_{z_{03}} + 3600\Omega_{z_{04}} - 1200\Omega_{z_{05}} + 300\Omega_{z_{06}} - 36\Omega_{z_{07}}}{720\Delta y} + O(\Delta y^5), \quad (16)$$

and for central points a centered approximation was adopted:

$$\frac{\partial \Omega_{z_0}}{\partial y} \Big|_{j-1} + 4 \frac{\partial \Omega_{z_0}}{\partial y} \Big|_j + \frac{\partial \Omega_{z_0}}{\partial y} \Big|_{j+1} = \frac{3\Omega_{z_{0j-1}} + 3\Omega_{z_{0j+1}}}{\Delta y} + O(\Delta y^4). \quad (17)$$

For the points at and next to the boundary of the opposite wall ( $y = 2$ ) the approximations (15) and (16) were used but with a sign inversion. After the  $U_0$  was calculated, then  $\Omega_{z_0}$  was calculated using the equation (14).

### 2.3.2. Temporal Integration

The temporal integration was done with an explicit 4th order Runge-Kutta method of four stages (Ferziger e Peric, 1997). The numerical procedure consisted of the following form: First the manufactured solution (in a time instant  $t = 0$ ), presented in the section 3, was introduced in the code as initial condition. Then for each stage of Runge-Kutta method, the following calculations were necessary:

1. Calculate the nonlinear terms  $A_k$  and  $B_k$  in the physical domain and transforms back to the Fourier space;
2. Calculate the right-hand side of the vorticity transport equation (8);
3. Integrate the vorticity transport equation in a stage;
4. Calculate the velocity  $V_k$  using the equation (9);
5. Calculate the wall vorticity  $\Omega_{z_k}$  ( $k \neq 0$ ) using the same equation (9).
6. calculate the velocity  $U_0$  and the vorticity at wall  $\Omega_{z_0}$  as described in the section 2.3.1.
7. Calculate the velocity  $U_k$  ( $k \neq 0$ ) using the equation (10).
8. Turn off to item 1 and repeat the above calculation until the time simulation expected.

As the Fourier modes were calculated independently, is not necessary the item 6 to be performed before item 7, it was done in this sequence only for a better organization of the numerical code routines.

### 3. The Verification Procedure: The Method of Manufactured Solutions

The current numerical code was verified using the Method of Manufactured Solutions (MMS). The chosen manufactured solution has the following form:

$$\begin{aligned} u(x, y) &= Ae^y y(y + 1 - \sqrt{5})(y + 1 + \sqrt{5})(y - 2) \cos(\alpha x - \omega t), \\ v(x, y) &= A \sin(\alpha x - \omega t) \alpha e^y y^2 (y^2 - 4y + 4), \\ \omega_z(x, y) &= -Ae^y \cos(\alpha x - \omega t) (8y^2 - 8 + 4\alpha^2 y^2 + \alpha^2 y^4 - 4\alpha^2 y^3 - 4y^3 + 8y - y^4). \end{aligned}$$

where  $A$  is an amplitude. The manufactured solution was produced using the following procedure: first, the  $u$ -component was chosen to satisfy the boundary conditions. The expression  $e^y$  that appear in  $u$  allows that the  $y$ -derivatives of any order were non-zero. The  $v$  was obtained using the continuity equation. For the  $v$  to satisfy the boundary conditions, the expressions  $(y + 1 - \sqrt{5})$  and  $(y + 1 + \sqrt{5})$  in  $u$  were necessaryes.  $\omega_z$  was then calculated from vorticity definition via Eq. (4). The requirement of nonzero  $y$ -derivatives allowed a systematic mesh refinement test for obtaining the order of accuracy of the code in the  $y$ -direction. Moreover the chosen manufactured solution oscillates in time with frequency  $\omega$  with a constant amplitude. It allowed to

imitate a neutral Tollmien-Schlichting wave that propagated in the flow direction in time with frequencies  $\omega$  and wavenumber  $\alpha$  along of a Poiseuille flow. Furthermore the chosen manufactured solution was not exponential in time to avoid confusion with numerical instability problem (Ethier e Steinman, 1994). The parameters  $\alpha$  and  $\omega$  were also made dimensionless by  $U_{max}$  and  $H$ . Therefore  $\alpha = \alpha^*H$  and  $\omega = \frac{\omega^*H}{U_{max}}$ .

Figure 2 shows the surfaces plot of  $u$ ,  $v$  and  $\omega_z$  of the manufactured solution and the energy spectrum of the Fourier modes in streamwise direction of the  $\Omega_z$ . The chosen parameters values were  $A = 5 \times 10^{-4}$ ,  $Re = 10^4$  and  $\alpha = \omega = 1$ . These parameters values were used when a long time simulation was performed. Contrary of the mesh refinement test, where the chosen Reynolds number and amplitude were  $A = Re = 1$ .

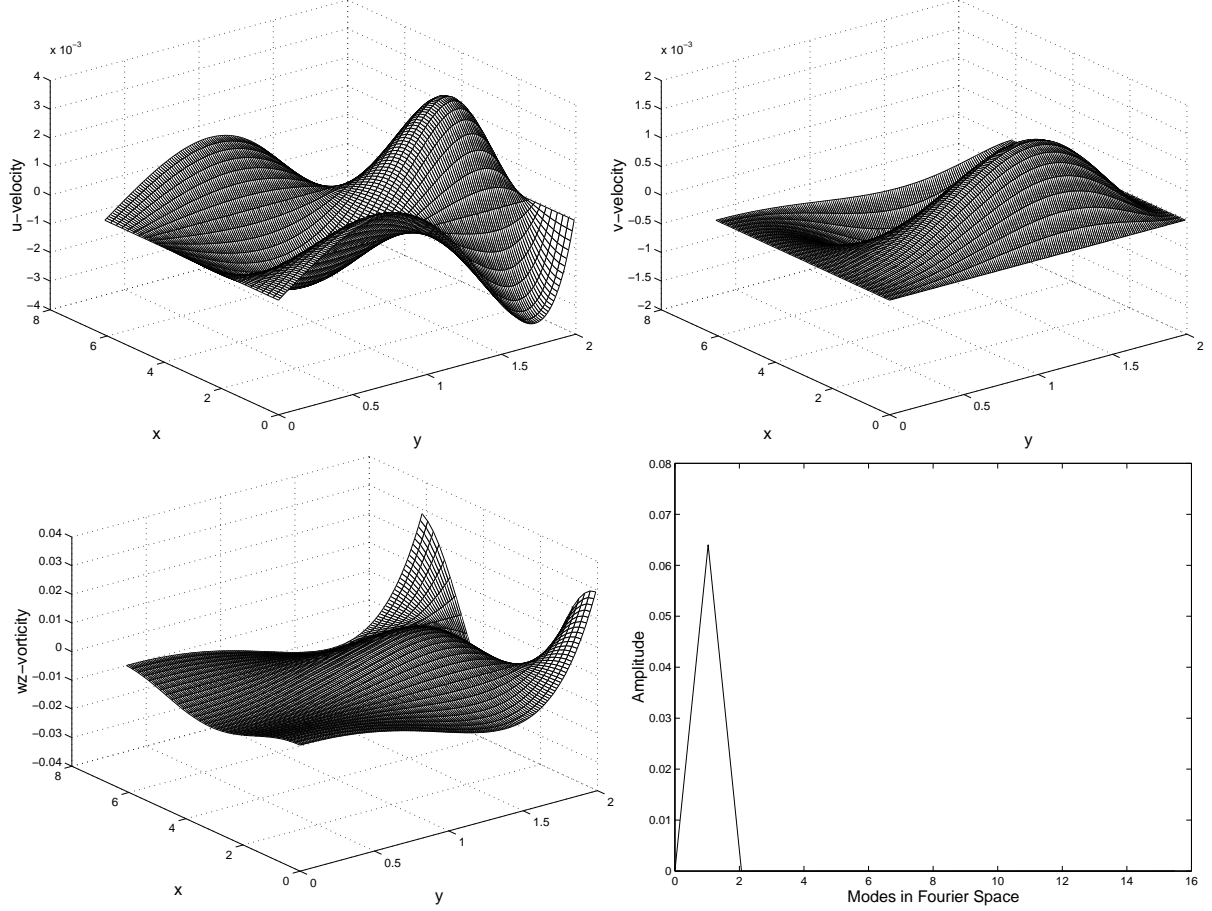


Figure 2: Surfaces plot of the chosen manufactured solution in the instant  $t = 0$ . This manufactured solution was used as initial condition for all the numerical simulations presented in the paper, but assuming different parameters values for each simulation.

The manufactured solution described above is analytical solution of the following fictitious problem:

$$\frac{\partial \omega}{\partial t} + \frac{\partial a}{\partial x} + \frac{\partial b}{\partial y} = \frac{1}{Re} \left( \frac{\partial^2 \omega}{\partial x^2} + \frac{\partial^2 \omega}{\partial y^2} \right) + Forc(x, y, t) \quad (18)$$

where the forcing term in physical space is

$$\begin{aligned} Forc(x, y, t) = & -(16\cos(\alpha x - \omega t)\alpha^2 y^2 - 8\sin(\alpha x - \omega t)\omega Re + 4\cos(\alpha x - \omega t)\alpha^4 y^2 + \\ & \cos(\alpha x - \omega t)\alpha^4 y^4 - 4\cos(\alpha x - \omega t)\alpha^4 y^3 - 8\cos(\alpha x - \omega t)\alpha^2 y^3 - 2\cos(\alpha x - \omega t)\alpha^2 y^4 + \\ & 18y^4 \sin(\alpha x - \omega t)\alpha Re + 8\sin(\alpha x - \omega t)\omega y Re + 12y^4 \sin(\alpha x - \omega t)\alpha^3 Re - \\ & 16y^2 \sin(\alpha x - \omega t)\alpha Re - 4\sin(\alpha x - \omega t)\omega Re y^3 - \\ & 8Ae^y y^4 \cos(\alpha x - \omega t)\sin(\alpha x - \omega t)\alpha Re + 64Ae^y y \cos(\alpha x - \omega t)\sin(\alpha x - \\ & \omega t)\alpha Re - 16y^3 \sin(\alpha x - \omega t)\alpha Re + 16y \sin(\alpha x - \omega t)\alpha Re - 8y^3 \sin(\alpha x - \omega t)\alpha^3 Re - \\ & 4\sin(\alpha x - \omega t)\omega Re \alpha^2 y^3 + 4\sin(\alpha x - \omega t)\omega Re \alpha^2 y^2 + \sin(\alpha x - \omega t)\omega Re \alpha^2 y^4 - \\ & 6y^5 \sin(\alpha x - \omega t)\alpha^3 Re + y^6 \sin(\alpha x - \omega t)\alpha^3 Re - 2y^5 \sin(\alpha x - \omega t)\alpha Re - \\ & y^6 \sin(\alpha x - \omega t)\alpha Re + \cos(\alpha x - \omega t)y^4 + 16\cos(\alpha x - \omega t)\alpha^2 y + \end{aligned}$$

$$\begin{aligned}
& 96Ae^y y^3 \cos(\alpha x - \omega t) \sin(\alpha x - \omega t) \alpha Re + \\
& 8Ae^y y^6 \cos(\alpha x - \omega t) \sin(\alpha x - \omega t) \alpha Re - \\
& 24Ae^y y^5 \cos(\alpha x - \omega t) \sin(\alpha x - \omega t) \alpha Re - \sin(\alpha x - \omega t) \omega Re y^4 - \\
& 128Ae^y y^2 \cos(\alpha x - \omega t) \sin(\alpha x - \omega t) \alpha Re + 28 \cos(\alpha x - \omega t) y^2 + \\
& 12 \cos(\alpha x - \omega t) y^3 - 16 \cos(\alpha x - \omega t) y - 16 \cos(\alpha x - \omega t) \alpha^2 - 24 \cos(\alpha x - \omega t) + \\
& 8 \sin(\alpha x - \omega t) \omega Re y^2) Ae^y / Re
\end{aligned}$$

The verification test was carried out of two different forms: first, as suggested by Roache, 1998, the order of accuracy of the code via a mesh refinement test in the  $y$ -direction using a small time simulation was performed. This simulation time was sufficient to the manufactured solution to migrate to numerical solution. After, numerical simulation of the manufactured solution using an infinitesimal amplitude  $A$  and it imitating a neutral Tolmien-Schilitching wave in the Poiseuille flow was performed, where a long time simulation was adopted. Contrary to the mesh refinement test that require, as suggested by Ethier e Steinman, 1994, simulation time very small to avoid truncation errors in time.

The mesh refinement test was realized using double precision in the calculations to avoid round-off error, the resolution in Fourier space was chosen to be  $\frac{2}{3}$  compared to the resolution in physical space to avoid aliasing error and a hundred time steps with time step ( $dt = 10^{-5}$ ) was the time simulation to avoid time truncation error. Therefore, the round-off error, aliasing error and time truncation error were negligible relative for the truncation error in  $y$ -direction. According to the above strategy, only the truncation errors relative to the  $y$ -direction calculations and possible programming errors predominated in the total numerical error. It was denoted by  $E_m$ . The mesh refinement test was made using the parameters  $A$  and  $Re$  set to 1 assuring that the terms of the studied equations have the same magnitude order (Roache, 1998). The total numerical error  $E_m$  is expressed by

$$E_m = |f_m - f_{exact}| \simeq g_p dy_m^p, \quad (19)$$

where  $f_m$  represents some numerical solution on mesh  $m$ ,  $f_{exact}$  represents the analytical solution of the chosen fictitious problem,  $g_p$  is the coefficient (dependent on high-order  $y$ -derivatives) of the leading error term and  $p$  is the order of accuracy. Applying the logarithmic function in equation (19) for the a finer mesh  $m$  and a coarser mesh  $m + 1$  it is possible to obtain the order of accuracy by using the following equation

$$\ln\left(\frac{E_{m+1}}{E_m}\right) = p \ln(r_m), \quad (20)$$

with  $r_m = \frac{dy_{m+1}}{dy_m}$ .

The order of accuracy for the present code was determined using six different meshes ( $m = 1, \dots, 6$ ) and the number of intervals doubled from one mesh to the following mesh. The first mesh used was  $dy = 0.25$  and the spatial domain in the  $y$ -direction was 2. This gives eight intervals in the  $y$ -direction.

Figures 3 to 5 show the behavior of the average and maximum absolute errors for  $u$ ,  $v$  and  $w_z$  respectively. The results were plotted in logarithmic scale. Fig. 3 and 4 show results where the straight line has a slope of 6 for both the mean and the maximum errors. On the other hand, Fig. 5 shows 6<sup>th</sup> order for the mean error and 5<sup>th</sup> order for the maximum error. The resultant 6<sup>th</sup> order for the maximum error occurred because the numerical error of the wall vorticity calculation is predominant over the numerical error in the interior of the domain. This predominance occurred principally because of the boundary condition calculation to  $\Omega_z$ , where the discretization scheme utilized the great values of the high order  $y$ -derivatives of  $\Omega_z$  in the wall points. More details on this issue can be found in Silva *et al.*, 2005. But, the resultant order was coherent with the theoretical order.

Despite the obtained order of accuracy was satisfactory, the manufactured solution as an infinitesimal disturbance in a long time simulation was also performed. The objective of this simulation was to verify if programming error increased in time. To the numerical solution of the equation (18) to imitate a neutral Tolmien-Schilitching wave in Poiseuille flow, the values of the parameters  $A$  and  $Re$  were  $5 \times 10^{-4}$  and  $10^4$  respectively. This manufactured solution only oscillates in time with constant amplitude and none solution deformation should appear after a long simulation time. The chosen time step for the present simulation was  $dt = 0.1454$  with 14400 time steps. This results in a total simulation time in turn of 90 cycles in time. Figure 6 shows the energy spectrum in Fourier domain of this manufactured solution after the time simulation above described. Comparisons between the numerical simulations with and without the primary Fourier mode calculation were realized. Note that there was a nonphysical energy quantitative in the primary Fourier mode when the primary Fourier mode calculation was performed. This occurred because there is a numerical instability problem in the primary Fourier mode calculation. The results of this simulation showed that the chosen solution scheme presented in the section 2.3.1 was not sufficient to eliminate the numerical instability in the primary Fourier mode calculation. In attempt to obtain greater stability for this calculation, a semi implicit scheme to the temporal integration of the wall normal diffusion terms will be implemented in the present code.

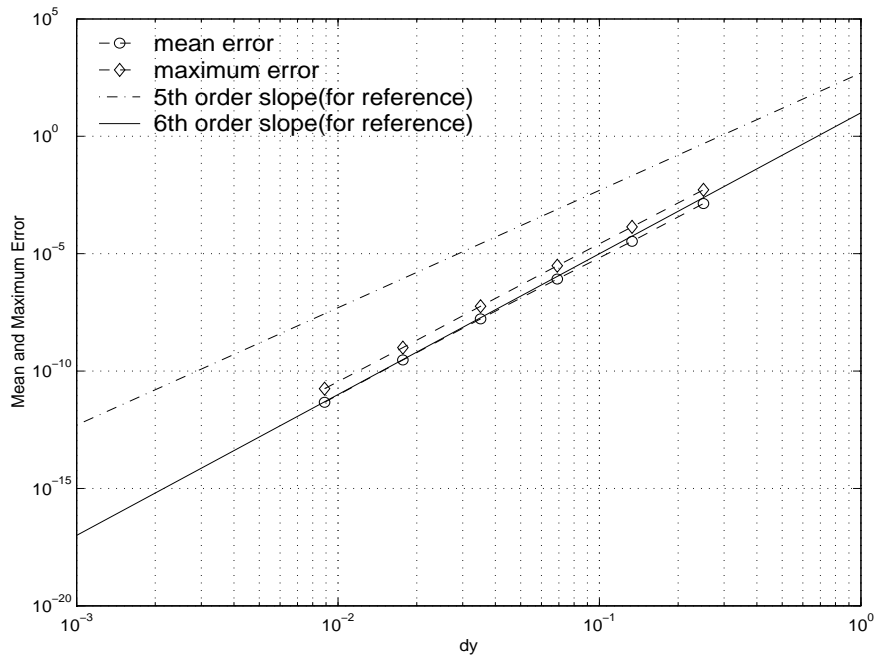


Figure 3: Behavior of the absolute mean and maximum errors  $E_m$  for the  $u$ -velocity.

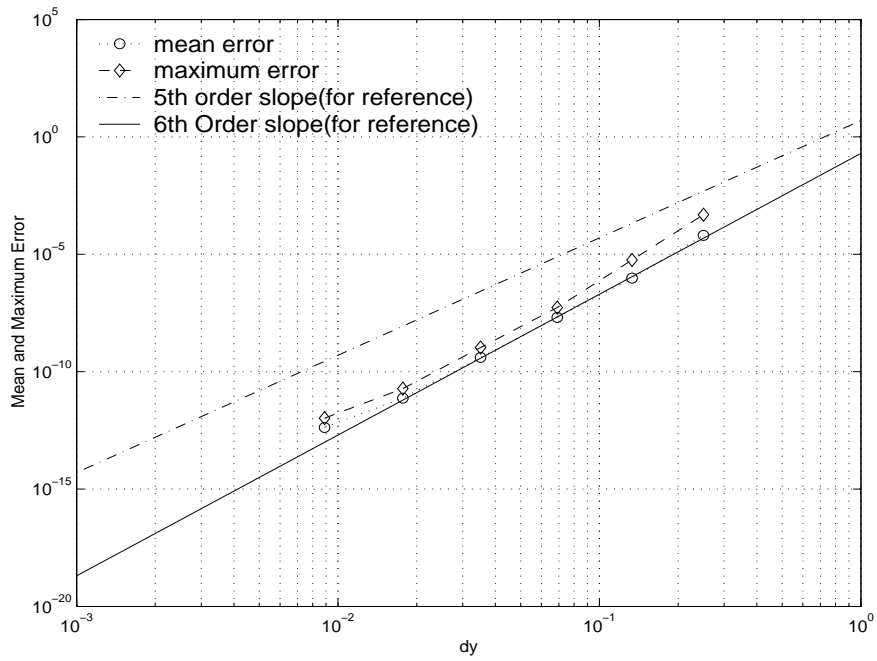


Figure 4: Behavior of the absolute mean and maximum errors  $E_m$  for the  $v$ -velocity.



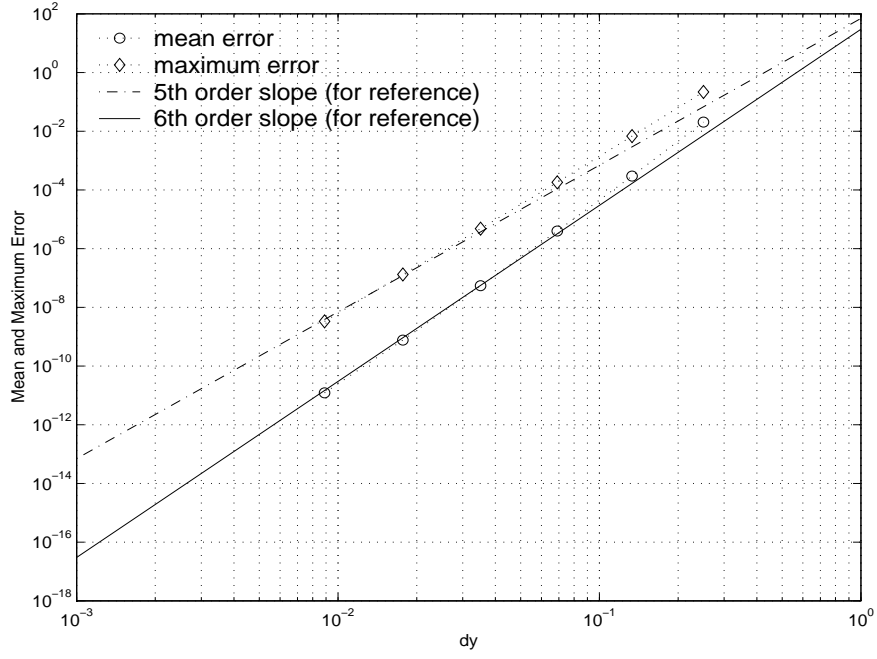


Figure 5: Behavior of the absolute mean and maximum errors  $E_m$  for the  $w_z$ -vorticity.

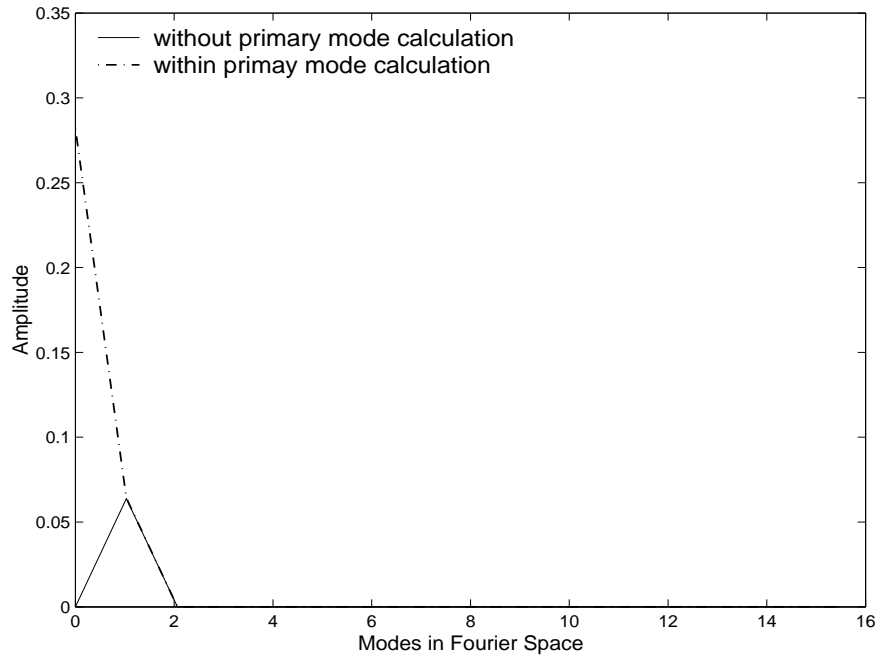


Figure 6: Comparison of the energy spectrum of  $w_z$  where the calculations were performed with (dashed line) and without (solid line) the primary Fourier mode calculation. Note the great amplitude of the primary Fourier mode presented by dashed line. The simulation time was in turn of 90 cycles in time.

## 4. Final Remarks

In the current work a verification test of a numerical code of high order of accuracy was presented. The verification test was done using the Method of Manufactured Solutions. Despite the MMS to be a general and very powerful approach to code verification, it was easy to obtain a manufactured solution that satisfied the boundary conditions yet implemented in the code without simplifications of the governing equations. Consequently, the nonlinear terms in the Navier-Stokes equations were also estimated. Contrary to others verification methods as comparison code-to-code or simulation of benchmark solutions, it was possible to exercise all of the terms in the equations and all of the leading error terms in the discretization scheme. The code verification was done using one test with a small time simulation and another test with a long time simulation. The test with a small simulation time was a mesh refinement test combined with order of accuracy verification. Since the discretization scheme used in this work had different orders of accuracy in the  $y$ -direction, depending on the grid position and on the equation, a lot of attention was required in the analysis of the results. Nevertheless, the resultant order was coherent with the theoretical order of the discretization scheme. For the  $u$  and  $v$ -components of velocity, the obtained order was six. But, to the spanwise vorticity  $\Omega_z$  the obtained order was five, due the discretization error from wall vorticity points was dominant compared with the discretization error from others points of the domain. Another important result was that the use of the average error is not a good technique for the study of the code order. Because it gave order six for the  $\Omega_z$  while that the maximum error technique gave order five. It helped to conclude that in the code order study, the analysis of the maximum error from chosen approximation scheme also is important.

The test with a long simulation time was also performed, using the same manufactured solution that was used to the code order analysis but with different parameters. The parameters  $A$ ,  $Re$ ,  $\alpha$  and  $\omega$  were chosen to the manufactured solution to imitate a neutral Tollmien-Schlichting wave propagating in a Poiseuille flow. It helped to identify if programming error increased in time. The results showed that a numerical instability appeared when the primary Fourier mode was calculated. But, the current numerical code had a good performance for the numerical simulations that despise it.

The numerical code will be used to simulate the temporal nonlinear development of modulated and unmodulated waves in a plane Poiseuille flow. Preliminary studies showed that the primary Fourier modes calculation can not have a strong relevance on the results of these future simulations. Therefore, the paper author's believe that numerical simulations without the primary Fourier modes calculation also will be proper to understand the behavior of the modulated and unmodulated waves in a plane Poiseuille flow in a highly nonlinear stage.

The code validation has been performed comparing the numerical simulation with primary and secondary stabilities results. Preliminary results of validation of the presented code can be found in Crepaldi *et al.*, 2006.

## 5. Acknowledgments

The financial support of the CNPq (Conselho Nacional de Desenvolvimento Científico e Tecnológico) and FAPESP (Fundação de Amparo à Pesquisa do Estado de São Paulo), grant 04/07507-4 are gratefully acknowledged.

## 6. Responsibility Notice

The authors are the only responsible for the printed material included in this paper.

## 7. References

- AIAA, 1994, Policy Statement on Numerical Accuracy and Experimental Uncertainty, "AIAA Journal", Vol. 32, pp. 3-3.
- ASME, 1994, Journal of Heat Transfer Editorial Policy Statment on Numerical Accuracy, "ASME Journal of Heat Transfer", Vol. 116, pp. 797-798.
- Crepaldi, F., Silva, H. G., Souza, L. F., and Medeiros, M. A. F., 2006, Temporal Numerical Simulation of Disturbances Propagation in a Poiseuille Flow Using Spectral Methods, "Escola de Primavera de Transição e Turbulência-EPTT", Vol. 1, Rio de Janeiro, Brazil.
- Ethier, C. R. and Steinman, D. A., 1994, Exact Fully 3-D Navier/Stokes Solutions for Benchmarking, "Int. J. Num. Meth. Fluids", Vol. 19, pp. 369-375.
- Ferziger, J. H. and Peric, M., 1997, "Computational Methods for Fluid Dynamics", Springer, Berlin, Germany.
- Freitas, C. J., 1993, Editorial Policy Statement on the Control of Numerical Accuracy, "ASME Journal of Fluids Engineering", Vol. 115, pp. 339-340.
- Gresho, P. M. and Taylor, C., 1994, editorial, "Int. J. Num. Meth. Fluids", Vol. 19, pp. 1-2.
- Marxen, O., 1998, "Temporal Numerical Simulation of a Flat Plate Boundary Layer", PhD thesis, University of Arizona, U.S.A.

- Roache, P. J., 1994, Response: To the Comments by Drs. W. Shyy and M. Sindir, "ASME Journal of Fluids Engineering", Vol. 116, pp. 198–199.
- Roache, P. J., 1997, Quantification of Uncertainty in Computational Fluid Dynamics, "Annu. Rev. Fluid. Mech.", Vol. 29, pp. 123–160.
- Roache, P. J., 1998, "Verification and Validation in Computational Science and Engineering", Hermosa Publishers, New México, USA.
- Roache, P. J. and White, F. M., 1986, Editorial Policy Statement on the Control of Numerical Accuracy, "ASME Journal of Fluids Engineering", Vol. 108, pp. 16–42.
- Shih, T. M., 1985, A Procedure to Debug Computer Programs, "Int. J. Num. Meth. Fluids", Vol. 21, pp. 1027–1037.
- Silva, H. G., Medeiros, M. A. F., and Souza, L. F., 2005, A Verification Test for a Direct Numerical Simulation Code that Uses a High Order Discretization Scheme, "18th International Congress of Mechanical Engineering, Proceedings of the COBEM", Ouro Preto, Brazil.
- Souza, L. F., Mendonça, M. T., and Medeiros, M. A. F., 2005, The Advantages of Using High-Order Finite Differences Schemes in Laminar-Turbulent Transition Studies, "Int. J. Num. Meth. Fluids", Vol. 48, pp. 565–582.
- Steinberg, S. and Roache, P. J., 1985, Symbolic Manipulation and Computational Fluid Dynamics, "Journal of Computational Physics", Vol. 30, pp. 251–283.